

RESEARCH ARTICLE

Open Access

Optimizing Bi_2O_3 and TiO_2 to achieve the maximum non-linear electrical property of ZnO low voltage varistor

Yadollah Abdollahi^{1*}, Azmi Zakaria^{1*}, Raba'ah Syahidah Aziz², Siti Norazilah Ahmad Tamili², Khamirul Amin Matori¹, Nuraine Mariana Mohd Shahrani², Nurhidayati Mohd Sidek², Masoumeh Dorraj¹ and Seyedehmaryam Moosavi²

Abstract

Background: In fabrication of ZnO-based low voltage varistor, Bi_2O_3 and TiO_2 have been used as former and grain growth enhancer factors respectively. Therefore, the molar ratio of the factors is quit important in the fabrication. In this paper, modeling and optimization of Bi_2O_3 and TiO_2 was carried out by response surface methodology to achieve maximized electrical properties. The fabrication was planned by central composite design using two variables and one response. To obtain actual responses, the design was performed in laboratory by the conventional methods of ceramics fabrication. The actual responses were fitted into a valid second order algebraic polynomial equation. Then the quadratic model was suggested by response surface methodology. The model was validated by analysis of variance which provided several evidences such as high F-value (153.6), very low P-value (<0.0001), adjusted R-squared (0.985) and predicted R-squared (0.947). Moreover, the lack of fit was not significant which means the model was significant.

Results: The model tracked the optimum of the additives in the design by using three dimension surface plots. In the optimum condition, the molars ratio of Bi_2O_3 and TiO_2 were obtained in a surface area around 1.25 point that maximized the nonlinear coefficient around 20 point. Moreover, the model predicted the optimum amount of the additives in desirable condition. In this case, the condition included minimum standard error (0.35) and maximum nonlinearity (20.03), while molar ratio of Bi_2O_3 (1.24 mol%) and TiO_2 (1.27 mol%) was in range. The condition as a solution was tested by further experiments for confirmation. As the experimental results showed, the obtained value of the non-linearity, 21.6, was quite close to the predicted model.

Conclusion: Response surface methodology has been successful for modeling and optimizing the additives such as Bi_2O_3 and TiO_2 of ZnO-based low voltage varistor to achieve maximized non-linearity properties.

Keywords: Optimization, ZnO-varistor, Modeling, RSM, Bi_2O_3 , TiO_2

Background

Varistors are nonlinear electro-devices with a ceramics microstructure that are used as protectors in distribution and energy transmission lines against voltage surge [1]. In the past four decades, varistors based on ZnO and SnO_2 have attracted attention because of their excellent non-ohmic behavior and low leakage currents [2,3].

However, ZnO-based varistor has been demanded along with the development of very-large-scale integration electronics because it exhibits high nonlinear current-voltage (I-V) characteristics in lower voltage ranges [4,5]. The non-linearity is expressed by $I = KV^\alpha$ where K is a constant, and ' α ' is nonlinear coefficient (alpha) [6]. The alpha originates from microstructure of the varistor ceramics which is composed of conductive n-type ZnO grains and small amount of a few metal oxide additives such as Bi_2O_3 , TiO_2 , Co_3O_4 , Mn_2O_3 , Sb_2O_3 and Al_2O_3 . The microstructure is made of ZnO grain surrounded by the melted additives as boundaries [4]. The boundaries

* Correspondence: yadollahabdolla@upm.edu.my; azmizak@science.upm.edu.my

¹Material Synthesis and Characterization Laboratory, Institute of Advanced Technology, Universiti Putra Malaysia, 43400 UPM, Serdang, Selangor, Malaysia

Full list of author information is available at the end of the article

contain of Bi-rich intergranular, metal oxide and secondary spinel phase and strictly influences on the alpha [4,6-11]. The role of Bi_2O_3 , as a former, is quite important since it provides the medium for liquid-phase sintering, enhances the growth of ZnO grains, and finally stables the nonlinear current-voltage characteristics of the varistor [12]. High sintering temperature is necessary for ZnO grain growth despite the fact that at this condition Bi_2O_3 tends to evaporate [13]. The melting point of Bi_2O_3 is 825°C , and the eutectic temperature of ZnO- Bi_2O_3 is only 740°C , thus a liquid phase is formed in the ZnO- Bi_2O_3 specimens below 800°C . As soon as the eutectic liquid is formed, the mass loss starts to increase which indicates the vaporization of Bi_2O_3 [14]. The sharp lost weight was reported above 1100°C since there was no reported peaks of $\beta\text{-Bi}_2\text{O}_3$ at 1300°C [15,16]. On the other hand, TiO_2 increases reactivity of the Bi_2O_3 -rich liquid phase with the solid ZnO during sintering process which prevents Bi_2O_3 vaporization [13,17-19]. The phase equilibrium and the temperature of liquid-phase formation are defined by the $\text{TiO}_2/\text{Bi}_2\text{O}_3$ ratio [20]. According to the reports, the effect of TiO_2 depends on Bi_2O_3 that means the additives interact in low-voltage varistor ceramics fabrication. To determine the effect of the interactions on the varistors' electrical properties, the molar ratios of the additives must simultaneously be considered. To the best of our knowledge, there is no study on the interactions which optimize the ratio of the additives and maximize the alpha. Recently, response surface methodology (RSM) has been accepted for modeling and optimizing of input intractable variables to achieve maximum yield product as output for productive process [21]. RSM is known as a semi-empirical

method because the process could be optimized by using experimental results, and a group of mathematical and statistical techniques [22]. In this work, RSM was used for modeling and optimizing of molar ratio of Bi_2O_3 and TiO_2 as additives to achieve the maximum value of the alpha for low voltage varistor. The experiments were designed by central composite design (CCD) to obtain the empirical results (actual). The results were used for regression and fitting process to fine an appropriate model. The model was verified by several statistical techniques such as residual analysis, scaling residuals and prediction error sum of squares (PRESS). The model optimized the input additives and then maximized the alpha as output. In addition, the model predicted the desirable condition including minimum standard error and the maximum alpha which are validated by further experiments. The predicted samples were characterized by X-ray diffractometer (XRD), scanning electron microscope (SEM), variable pressure scanning electron microscope (VPSEM) and Energy-dispersive X-ray (EDX).

Experimental

Materials and methods

The commercial chemical, ZnO (99.99%), Bi_2O_3 (99.975%), TiO_2 (99.9%), Sb_2O_3 (99.6%), Mn_3O_4 (98%), Co_3O_4 (99.7%) and $\text{Al}(\text{NO}_3)_3$ (100% ± 2), were provided from Alfa Aesar as starting powders. The powders were weighed according to the experimental design of molar ratios (Table 1). The molar ratios of the powders were mixed, ground in dry form and then ball milled in acetone for 24 h. During ball milling, agglomeration was controlled by Zirconium oxide balls. After drying in hot oven for 8 h, the mixed powders were grounded and pressed into pellet forms of 10 mm in

Table 1 Experimental-design contain of the actual variables, and actual response and model predicted values of the alpha

Run	ZnO	TiO_2	Bi_2O_3	Co_3O_4	Mn_2O_3	Sb_2O_3	$\text{Al}(\text{NO}_3)_3$	Alpha (Actual)	Alpha (Predicted)
1	96.50	1	1	0.5	0.5	0.5	0.00094	9.3	10.1
2	96.00	1.5	1	0.5	0.5	0.5	0.00094	3.9	3.9
3	96.00	1	1.5	0.5	0.5	0.5	0.00094	6.4	7.4
4	95.50	1.5	1.5	0.5	0.5	0.5	0.00094	10.5	10.6
5	96.35	0.896	1.25	0.5	0.5	0.5	0.00094	9	7.9
6	95.65	1.604	1.25	0.5	0.5	0.5	0.00094	5.6	5.8
7	96.35	1.25	0.896	0.5	0.5	0.5	0.00094	8.2	7.7
8	95.65	1.25	1.604	0.5	0.5	0.5	0.00094	11	10.5
9	96.00	1.25	1.25	0.5	0.5	0.5	0.00094	20	20
10	96.00	1.25	1.25	0.5	0.5	0.5	0.00094	19.6	20
11	96.00	1.25	1.25	0.5	0.5	0.5	0.00094	20.2	20
12	96.00	1.25	1.25	0.5	0.5	0.5	0.00094	20.7	20
13	96.00	1.25	1.25	0.5	0.5	0.5	0.00094	19.4	20

diameter and 0.70 mm thickness at 200 MPa by a uniaxial presser machine. The disks were sintered in a box furnace (CMTS Model HTS 1400) for holding time of 2 h at 1260°C. The heating and cooling rate were 5°C/min [23]. To determine DC current-voltage (I-V), both of the sintered sample surfaces were coated by silver electrodes. The I-V of the samples was measured by Keithley 236 source meter. The samples were scanned with dc voltage from 0 to 100 V in step size of 2.5 V. The alpha was calculated at $J_1 = 0.1$ and $J_2 = 1$ mA/cm² by equation (1) as actual responses [6].

$$\alpha = (\log J_2 - \log J_1) / (\log E_2 - \log E_1) \quad (1)$$

The breakdown voltage (E_b) was determined by measuring E at $J = 0.75$ mA/cm² and the leakage current (J_L) was determined evaluating J at $0.8E_b$ where J (mA/cm²) is the current density and E is the electrical field (V/mm). To characterize the microstructure, the both surfaces of samples were polished by aluminum oxide powder. Then, they were etched at 160°C under sintering time with heating and cooling rate, 10°C/min. Phase analysis was conducted using XRD (PANalytical, Philips-X'pert Pro PW3040/60) with CuK α source. The sample were radiated with Ni-filtered CuK α radiation ($\lambda = 1.5428$) within the 2 θ scan range of 20–80°. Surface morphology and elemental analyses of sintered samples were studied under SEM (JEOL JSM 6400) and VPSEM (LEO 1455) which attached to EDX. The samples was mounted on Al stub using carbon paint and coated by gold layer. Average grains size of the ZnO in the varistor was evaluated by measuring 100 grains in SEMs images.

Experimental design

The experimental design was carried out by CCD that used Design-Expert software version 8.0.7.1, Stat-Ease Inc., USA [24-26]. CCD is well fixed for fitting a quadratic surface that usually works well for optimization process [27-29]. The variables number, level of variables and number of responses are determined as input of experimental design. In this case, the molar ratio of Bi₂O₃ and TiO₂ was selected as effective variables in vicinity of their optimum while alpha was the response as output. The CCD transformed the variables and the response to the terms of code values (Table 2) because the units and range of variables were different. The coded values

spaces are ± 1 from the center (0.0) and the star points are usually located ' α ' distance from the center [29,30]. In the design, there N experiment that includes the factorial points (2^n), the axial points (2n), and the center points C_o or replications as the equation $N = 2^n + 2n + C_o$ which is 13, 4, 4 and 5 respectively. The replications are used to measure experimental error [31]. As a result, the experimental design is presented as a design matrix with 'n' column and 'N' row in Table 1. Where, each column corresponds to a particular variable, e.g. x_1 and x_2 which arranged in order to increase factor number from left to right. The rows are experiments runs because each one contains the descriptions of an experiment. Additionally, the design constructs a matrix of actual responses that obtained by the experiments.

The RSM description

The RSM develops an adequate functional relationship between input variables and interested responses by low-degree approximation of the polynomial models such as the second degree model (Eq. 2) [32].

$$Y = \beta_o + \sum_{i=1}^n \beta_i x_i + \sum_{i=1}^n \beta_{ii} x_i^2 + \sum_{i=1}^n \sum_{j=i+1}^n \beta_{ij} x_i x_j + \varepsilon \quad (2)$$

where Y is the interested response, β_o is the constant term, β_i is the coefficient of the linear terms, β_{ii} represents the coefficient of the quadratic terms, β_{ij} is the coefficient of the interaction terms while x_i are control variables and ' ε ' is a random experimental error [31]. For system with two factors, the model is described by equation (3),

$$Y_{1i} = \beta_o + \beta_1 x_{1i} + \beta_{11} x_{1i}^2 + \beta_{22} x_{2i}^2 + \beta_{12} x_{1i} x_{2i} + r_{1i} \quad (3)$$

where Y_{1i} is the experimental single response, x_1 and x_2 are the coded factors (Table 2), β_o is the intercept term, β_1 and β_2 are slopes with respect to each of the two factors, β_{11} and β_{22} are curvature terms, and β_{12} is the interaction term. To estimate the β 's, the fitting process provides the sufficient data by regression tools [33,34]. In the process, the actual responses are fitted to the polynomial models by sequential model sum of squares (SMSS) [33,34]. The SMSS compares the linear, two-factor interaction (2FI), quadratic and cubic models by using the statistical significance of adding new model terms, step by step in increasing order [35]. To select the provisional model, the lack of fit of those models is compared by minimum p-values and PRESS. The other assessments to select

Table 2 The variables and employed levels in the CCD for ZnO low voltage varistor fabrication

Symbol	Unit (%)	Level of variables		
		Low (-1)	Middle (0)	High (+1)
Bi ₂ O ₃ (x_1)	mol	1.0	1.25	1.5
TiO ₂ (x_2)	mol	1.0	1.25	1.5

the best provisional model are maximum adjusted R-squared (R_{Adj}) and predicted R-squared (R_{Pred}) [36]. The p-value is one of the most important evidences which was used to study significant effect of the parameters [33]. In addition, the lack-of-fit test diagnoses how well each terms of the full model fit the data that pillared by statistical parameters such as R_{Adj} , R_{Pred} and PRESS [36,37]. Therefore, the provisional model with minimum p-value and PRESS and also maximum R_{Adj} , R_{Pred} is selected to investigate in details. The details are provided by using analysis of variance (ANOVA) which contains a collection of terms statistical evidences. The ANOVA determines the significance of intercept, linear, interaction and square terms of the provisional model by using minimum p-value. For more evaluation, the normality of residuals, constant error and residual outlier is checked by various diagnostic plots [38]. The validated model, the relationship between variables and response, is created in coded and actual variables. The model indicates the effect of linear, quadratic and the parameters interactions on the interested response. The effects are presented by estimated coefficients and the related positive and negative signs (+, -). The coefficients are specific weight of the parameters in the model while the signs (+) and (-) operate as synergistic and antagonistic effects on the response [39]. Then the optimization process investigates combination of variables levels that produces the maximum response to a surface area simultaneously. Moreover, the model predicts the yield of product in specific condition such as individual standard error, the range of variables and responses. The prediction could be performed by further experiments.

Results and discussion

Modeling

In the fitting process, the residuals are produced from difference between actual and predicted values. Standard error is a great tool to determine the residuals outlier and also the scope of models prediction [40]. Figure 1 indicates the standard error contour plot of the experimental design which displays Bi_2O_3 versus TiO_2 molar ratio. The bright area has relatively low standard error that interested for the modeling and optimization process. However, the darker shading corners represent higher standard errors which are dangerous to extrapolation.

Table 3 indicates that the SMSS compared four models to recommend a proper model [35,36]. As shown, the quadratic model was suggested as the best provisional model. The suggestion based on the lowest standard deviation, p-value and PRESS and the highest R_{Adj} , R_{Pred} values. Moreover, the R_{Adj} (0.991) was in reasonable agreement with (<0.20) R_{Pred} (0.985) which confirmed the model sufficiency. Therefore, the authors selected the suggested model to investigate in details by using ANOVA.

Table 4 shows the ANOVA of the provisional model which included the useful statistical evidences about the terms (x_1 , x_2 , $x_1 x_2$, x_1^2 and x_2^2) in details. As shown, the prob > F of the terms was less than 0.05 which confirmed the high significance of the terms. Moreover, the model's F-value was 153.6 that indicated great significance for the model. In addition, the very low value of the model p-value confirmed the significance. Furthermore, R-squared (R) provides a measure of how much variability in the observed response values

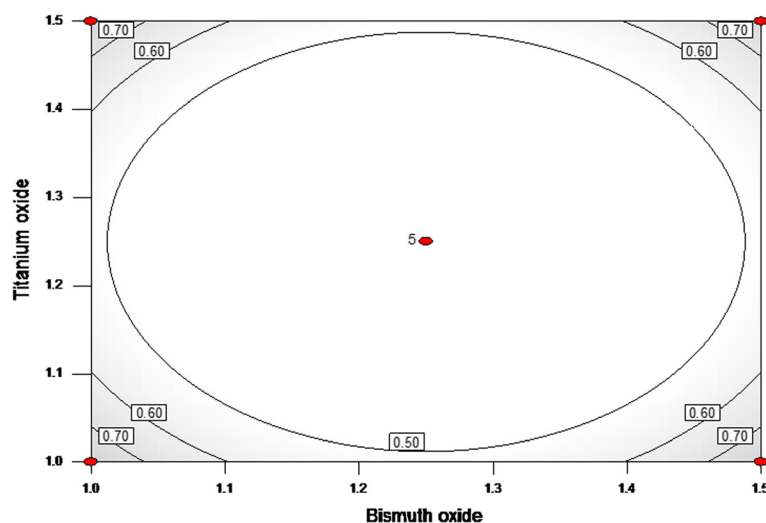


Figure 1 Contour plot of the experimental-design standard error with expanded axes, extrapolated area shaded.

Table 3 The sequential model fitting summary for the actual responses which shows statistics conformation of the regression process, DF is degree of freedom

Source	Sum of squares	DF	Mean square	F-Value	p-value	Remark
Sequential model sum of squares						
Mean vs Total	2064.18	1	2064.18	-	-	
Linear vs Mean	12.07	2	6.04	0.13	0.8818	
2FI vs Linear	22.31	1	22.31	0.44	0.5216	
Quadratic vs 2FI	447.11	2	223.55	356.58	< 0.0001	Suggested
Cubic vs Quadratic	1.56	2	0.78	1.38	0.3325	Aliased
Residual	2.83	5	0.57	-	-	
Total	2550.06	13	196.16	-	-	
Source	Sum of squares	DF	Mean square	F-Value	p-value	Remark
Lack of fit tests						
Linear	472.78	6	78.80	307.73	< 0.0001	
2FI	450.47	5	90.09	351.85	< 0.0001	
Quadratic	3.36	3	1.12	4.38	0.0938	Suggested
Cubic	1.80	1	1.80	7.03	0.0569	Aliased
Pure Error	1.02	4	0.26	-	-	
Source	Std.Dev.	R _{Adj}	R _{Pred}	R	PRESS	Remark
Model summary statistics						
Linear	6.88	0.025	-0.170	-0.571	763.55	
2FI	7.08	0.071	-0.239	-1.195	1066.45	
Quadratic	0.79	0.991	0.985	0.947	25.53	Suggested
Cubic	0.75	0.994	0.986	0.760	116.85	Aliased

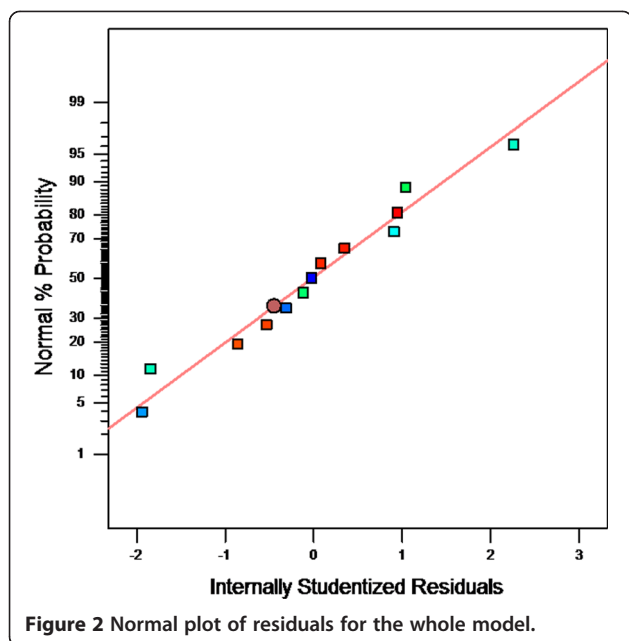
can be explained by the experimental factors and their interactions. In this study, the R (0.991) indicated that the model was capable of accounting for more than 99.1% of the variability in the responses. The R_{Adj} (0.985) was in reasonable agreement with (<0.20) the R_{Pred} (0.947) which confirmed the aptness of the model. The pure errors such as experimental errors were minimal as the lack of fit

(0.094) was not significant or the model was fit well. Therefore, ANOVA confirmed the adequacy of the quadratic model that could be used to navigate the design space.

The normality of residuals, constant error and residual outliers were checked by various diagnostic plots. The normal probability plots of the studentized residuals as one of the most important diagnostic plots, was provided

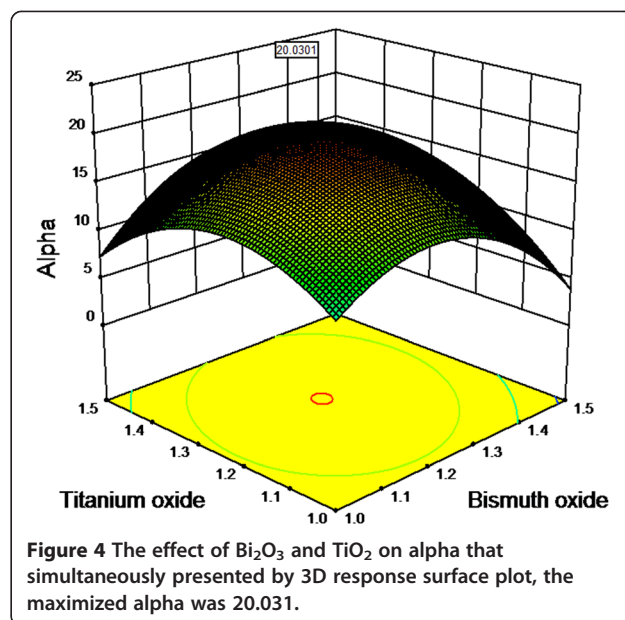
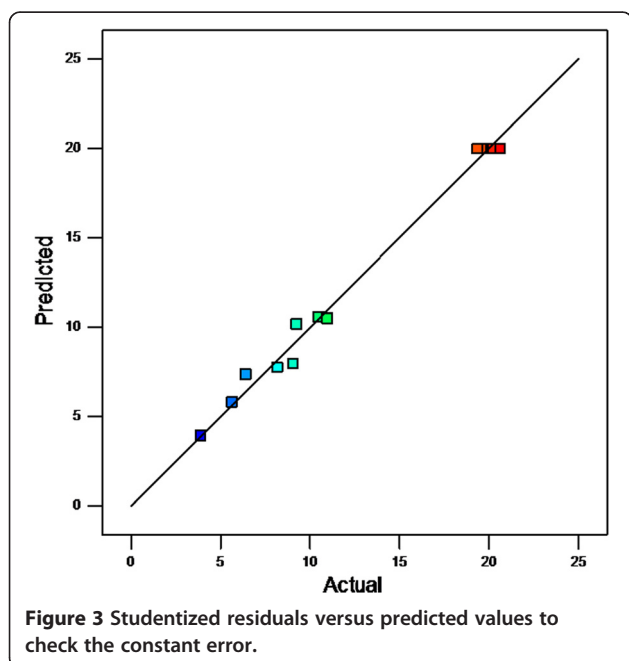
Table 4 Analysis of variance (ANOVA) for response surface quadratic model, MS is mean Square, DF is degree of freedom and SS is sum of squares while x₁ and x₂ introduce in Table 2

Source	SS	DF	MS	F-Value	p-value (Prob > F)	Suggestion
Model	481.5	5	96.3	153.6	< 0.0001	significant
x ₁	4.6	1	4.6	7.4	0.0299	
x ₂	7.4	1	7.4	11.9	0.0108	
x ₁ x ₂	22.3	1	22.3	35.6	0.0006	
x ₁ ²	298.7	1	298.7	476.4	< 0.0001	
x ₂ ²	205.5	1	205.5	327.7	< 0.0001	
Residual	4.4	7	0.6			
Lack of Fit	3.4	3	1.1	4.4	0.0938	not significant
Pure Error	1.0	4	0.3		< 0.0001	
Cor Total	485.9	12			0.0299	
Std.Dev.	R _{Adj}	R _{Pred}	R ²	PRESS	C.V.%	Adeq Precision
0.792	0.985	0.947	0.991	25.5	6.284	29.9



by software default (Figure 2). The plot presents percentage of normal% probability versus internal studentized residuals. The studentized residual is an important technique in the detection of residuals outliers in regressions [41]. As the plot demonstrates, the residuals followed a normal distribution that implies the points follow a straight line.

As another diagnosis, Figure 3 illustrates the predicted response values versus the actual response values and detects the values that are not easily predicted by the model. The data points were on the 45 degree line that



means the values were not detected. As a result, the diagnosis of residuals reveals that there is no statistical problem in the model.

The model presentation

The model expresses the relationship between responses of actual variables and the variables themselves. The validated model is presented in actual variables by equation (4),

$$Y = -221.67 + 211.82x_1 + 174.00x_2 + 37.79x_1x_2 - 104.84x_1^2 - 86.95x_2^2 \quad (4)$$

where the actual values of the variables x_1 and x_2 were shown in Table 2 and Y is the alpha. As shown, the parameters including linear (x_1 , x_2), quadratic (x_1^2 , x_2^2) and interaction (x_1x_2) affected on the interested response. The effects are presented by the individual coefficients and the related signs (+, -) in the model. The coefficients indicate the specific weight of the parameters in the model while the signs are synergistic (+) and antagonistic (-) effects of variables on the response (Y).

Table 5 The summary of optimized input variables and obtained maximized alpha% by canonical, graphical, numerical methods and validation value of the photodegradation

Method	Bi_2O_3 (%mol)	TiO_2 (%mol)	Alpha
Canonical (point)	1.195	1.025	15.03
Graphical (area)	Area around 1.25	Area around 1.25	20.03
Numerical (prediction)	1.24	1.27	20.03
Validated sample	1.24	1.27	21.6

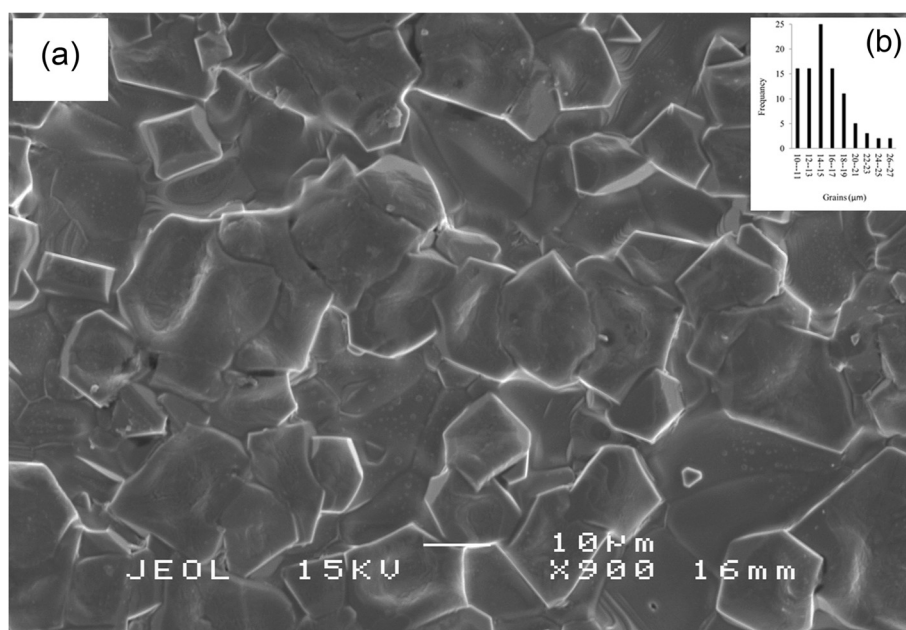


Figure 5 The microstructure of the optimized varistor morphology, (a) SEM (b) distribution of ZnO grain size.

The weights determine the importance of the parameters roles in the modeling. The model is able to optimize input variables and also approximately predict the response inside of the actual experimental region that confirmed by minimum standard error (Figure 1) [33]. Therefore, the model was used to optimize the molar ratio of Bi_2O_3 and TiO_2 to achieve maximized alpha.

The model optimization

The model is able to optimize the variables by using canonical response and graphical plots. The canonical responses, local optimums, in terms of the code and actual

variables were determined by differentiating the model (Eq. 4) as presented in equations (5 and 6),

$$[\partial Y / \partial x_1]_{x_2} = 0 \quad (5)$$

$$[\partial Y / \partial x_2]_{x_1} = 0 \quad (6)$$

where the terms were introduced in Table 2. Therefore, the optimum canonical amount of Bi_2O_3 and TiO_2 were 1.195 and 1.025 respectively. At this optimum, the maximized alpha was 15.03. In fact, the optimization is a kind of the traditional methods, one-variable-at-a-time, because in each case, one of the variables was varied and

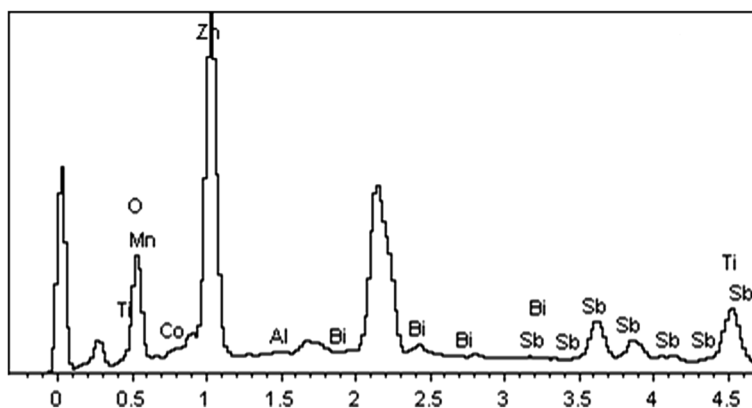


Figure 6 The EDX of etched optimized sample surfaces.

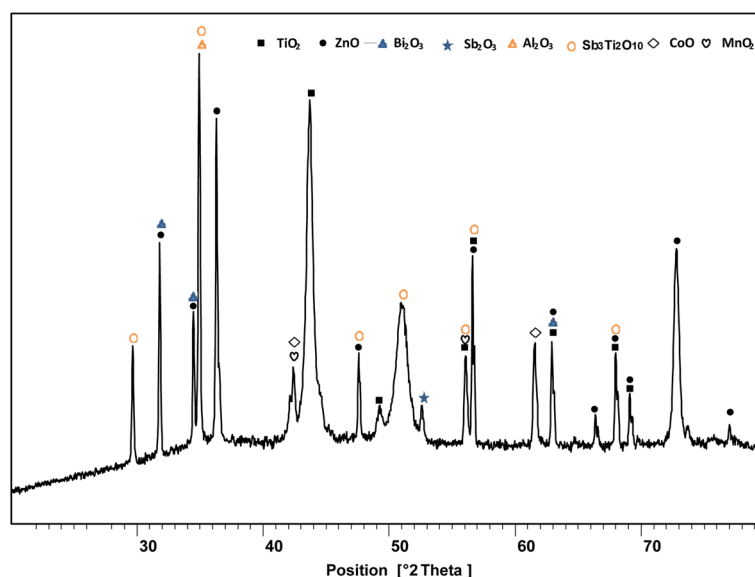


Figure 7 The XRD patterns of optimized varistor sample which include ZnO, additives and spinel.

others were constant. In graphical optimization, the model simultaneously considered the effect of Bi_2O_3 and TiO_2 on the alpha. Figure 4 presents the three dimension response surface (3D) plot for the synergy between Bi_2O_3 (1–1.5 mol%) and TiO_2 (1–1.5 mol%) which is standard error limitation area (Figure 1). As shown, the alpha increased within 1 to 1.25 mol% Bi_2O_3 and TiO_2 . However, when the amount of Bi_2O_3 and TiO_2 was increased in excess of the optimum (1.25 mol%), the alpha decreased. Therefore, the optimum was determined in a surface area around 1.25 mol% for the both additives. The maximum alpha was 20.031 at center of the surface which indicated by a flag on top of Figure 4.

The model predicted the maximized alpha in desirable condition of the additives and standard error which facilitated by default of software numerical option. The desirability is an objective function that uses mathematical methods to find the optimum condition [25]. The range of the function is from zero (outside of the limit area) to one (at the goal). The criteria for this case Bi_2O_3 (in range), TiO_2 (in range), standard error (minimized) and alpha (maximized). The suggested solution was Bi_2O_3 (1.24 mol%), TiO_2 (1.27 mol%), standard error (0.35), and alpha 20.03. The desirability of the solution was 0.981 which is close to 100% (at the goal). The solution was performed to confirm the prediction by validated experiment. The validated alpha was determined 21.6 which was quite close to the predicted alpha (20.03). Table 5 illustrated a summary of optimized molar ratios of Bi_2O_3 and TiO_2 and also the related maximized alpha which obtained by canonical, graphical and numerical model optimization method.

The validated varistor

The validated sample was characterized as final varistor for this optimization process. Figure 5 demonstrates the SEM morphology of the sintered ceramic microstructure of the varistor. Figure 5a indicates the great homogeneity of ZnO grain size. The average grain size was 15 μm (Figure 5b).

Figure 6 illustrates EDX spectra of a limited area of the etched varistor surfaces composition. As shown all additives particular Bi (1.0 weight%) and Ti (1.17 weight%) were detected in the selected area after sintering process at 1260°C.

Figure 7 shows the XRD pattern of the optimized sample which presented three phase of ZnO, spinel and metal

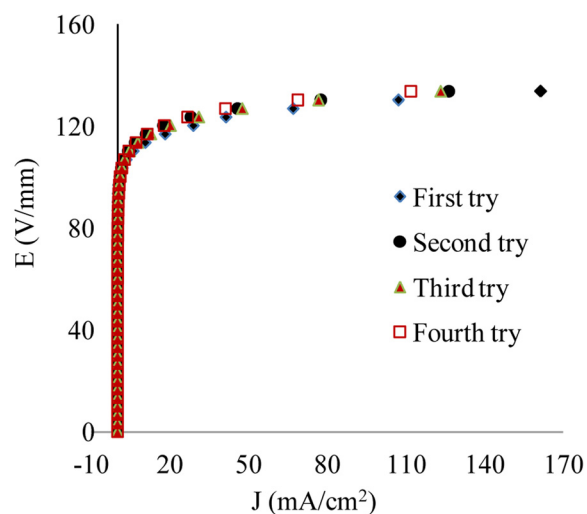


Figure 8 E-J characteristic curves of the optimized samples for first to fourth measurements.

oxide of additives. The composites were including ZnO (00-005-0664), Bi₂O₃ (00-002-0988), TiO₂ (01-072-0020), MnO₂ (00-003-1041), CoO (00-048-1719), Sb₂O₃ (01-075-1567), Al₂O₃ (00-004-0879) and Sb₃Ti₂O₁₀ (00-028-0103). The number that mentioned in parenthesis are XRD reference code.

The electrical properties of the varistor were basis of I-V characteristic measurement that shows breakdown voltage was 98 V/mm with non-linear coefficient 21.6. The leakage current was 0.013 mA/cm². The stability of the varistor was measured by alpha recovery after removing the over voltage (Figure 8). As shown the stability was quit significant after fourth over voltage.

Conclusions

This work reports modeling and optimization of the molar ratio of Bi₂O₃ and TiO₂ by RSM. The fabrication was designed by CCD using two variables and a response. To obtain actual responses, the design was performed in laboratory by conventional fabrication methods. The actual responses were fitted into a quadratic model. The model was validated by ANOVA which provided evidences such as high F-value (153.6), very low p-value (<0.0001), R_{adj} (0.985) and R_{pred} (0.947). The results of the validation showed the model was significant. The model tracked the optimum of the designed additives by using 3D plots. In the optimum condition, the molar ratio of Bi₂O₃ and TiO₂ were around 1.25 that maximized the alpha value at 20. Moreover, the model suggested a solution to predict the optimum amount of the additives. In this case, the condition of the solution included standard error of 0.35, Bi₂O₃ of 1.24, TiO₂ of 1.27 and alpha of 20.03. The solution was tested by further experiments. As the validation test showed, the obtained value of the alpha (21.6) was very close to the predicted value (20.03). Therefore, RSM was succeeded in modeling of the additives in fabrication of zinc oxide based low voltage varistor to achieve maximum alpha.

Competing interests

The authors declare that they have no competing interests.

Authors' contributions

YA carried out the catalyst design and ligand screening studies. YA, SNA-T, NMM-S and NMS carried out the synthesis, purification and characterization of the compounds. YA carried out the computational experiments. AZ, RSA and KAM conceived of the study, and participated in its design and coordination and helped to draft the manuscript. All authors read and approved the final manuscript.

Acknowledgements

The author would like to express acknowledgement to Ministry of Higher Education Malaysia for granting this project under Research University Grant Scheme (RUGS) of Project No. 05-02-12-1878. The authors wish to thank Dr Pedram Lalbakhsh for polishing and proofreading the manuscript.

Author details

¹Material Synthesis and Characterization Laboratory, Institute of Advanced Technology, Universiti Putra Malaysia, 43400 UPM, Serdang, Selangor,

Malaysia. ²Department of Physics, Faculty Science, Universiti Putra Malaysia, 43400 UPM, Serdang, Selangor, Malaysia.

Received: 19 May 2013 Accepted: 6 August 2013

Published: 10 August 2013

References

- Ramírez M, Bueno P, Ribeiro W, Varela J, Bonett D, Villa J, Márquez M, Rojo C: **The failure analyses on ZnO varistors used in high tension devices.** *J Mater Sci* 2005, **40**:5591–5596.
- Ramírez M, Bassi W, Bueno P, Longo E, Varela J: **Comparative degradation of ZnO-and SnO₂-based polycrystalline non-ohmic devices by current pulse stress.** *J Phys D Appl Phys* 2008, **41**:122002–122002.
- Ramírez MA, Bassi W, Parra R, Bueno PR, Longo E, Varela JA: **Comparative electrical behavior at low and high current of SnO₂ and ZnO based varistors.** *J Am Ceram Soc* 2008, **91**:2402–2404.
- Levinson L, Philipp H: **Zinc oxide varistors—a review.** *Am Ceram Soc Bull* 1986, **65**:639.
- Eda K: **Zinc oxide varistors.** *IEEE Electr Insul Mag* 2002, **5**:28–30.
- Bernik S, Zupancic P, Kolar D: **Influence of Bi₂O₃/TiO₂/Sb₂O₃ and Cr₂O₃ doping on low-voltage varistor ceramics.** *J Eur Ceram Soc* 1999, **19**:709–713.
- Suzuki H, Bradt R: **Grain growth of ZnO in ZnO-Bi₂O₃ ceramics with TiO₂ addition.** *J Am Ceram Soc* 1995, **78**:1354–1360.
- Clarke DR: **Varistor ceramics.** *J Am Ceram Soc* 1999, **82**:485–502.
- Pillai SC, Kelly JM, McCormack DE, O'Brien P, Ramesh R: **The effect of processing conditions on varistors prepared from nanocrystalline ZnO.** *J Mater Chem* 2003, **13**:2586–2590.
- Elfving M, Österlund R, Olsson E: **Differences in wetting characteristics of Bi₂O₃ polymorphs in ZnO varistor materials.** *J Am Ceram Soc* 2000, **83**:2311–2314.
- Lao Y-W, Kuo S-T, Tuan W-H: **Effect of Bi₂O₃ and Sb₂O₃ on the grain size distribution of ZnO.** *J Electroceram* 2007, **19**:187–194.
- Peiteado M, Fernández Lozano JF, Caballero AC: **Varistors based in the ZnO-Bi₂O₃ system: microstructure control and properties.** *J Eur Ceram Soc* 2007, **27**:3867–3872.
- Peiteado M, De la Rubia M, Velasco M, Valle F, Caballero A: **Bi₂O₃ vaporization from ZnO-based varistors.** *J Eur Ceram Soc* 2005, **25**:1675–1680.
- Metz R, Delalu H, Vignalou J, Achard N, Elkhatib M: **Electrical properties of varistors in relation to their true bismuth composition after sintering.** *Mater Chem Phys* 2000, **63**:157–162.
- Wong J: **Sintering and varistor characteristics of ZnO Bi₂O₃ ceramics.** *J Appl Phys* 1980, **51**:4453–4459.
- Yilmaz S, Ercen E, Toplan HO, Gunay V: **Grain growth kinetic in x TiO₂-2-6 wt.% Bi₂O₃-(94-x) ZnO (x = 0, 2, 4) ceramic system.** *J Mater Sci* 2007, **42**:5188–5195.
- Toplan HO, Karakaş Y: **Processing and phase evolution in low voltage varistor prepared by chemical processing.** *Ceram Int* 2001, **27**:761–765.
- Yan MF, Heuer AH: **Additives and interfaces in electronic ceramics.** Columbus, OH: Amer Ceramic Society; 1983.
- Peigney A, Andrianjatovo H, Legros R, Rousset A: **Influence of chemical composition on sintering of bismuth-titanium-doped zinc oxide.** *J Mater Sci* 1992, **27**:2397–2405.
- Bernik S, Daneu N, Rečnik A: **Inversion boundary induced grain growth in TiO₂ or Sb₂O₃ doped ZnO-based varistor ceramics.** *J Eur Ceram Soc* 2004, **24**:3703–3708.
- Montgomery DC: **Design and analysis of experiments.** New York: John Wiley & Sons Inc; 2008.
- Khuri AI, Cornell JA: **Response surfaces: designs and analyses.** New York: CRC; 1996.
- Bernik S: **Microstructural and electrical characteristics of ZnO based varistor ceramics with varying TiO₂/Bi₂O₃ ratio.** In *Advances in science and technology*; 1999:151–158.
- Williges RC, Clark C: **Response surface methodology design variants useful in human performance research,** Illinois Univ Savoy Aviation Research Lab; 1971.
- Myers RH, Anderson-Cook CM: **Response surface methodology: process and product optimization using designed experiments.** New Jersey: John Wiley and Sons, Inc; 2009.

26. Clark C, Williges RC: *Response surface methodology design variants useful in human performance research*, DTIC Document, New York; 1971.
27. Deming S: **Quality by design-part 5**. *Chemtech* 1990, **20**:118–120.
28. Hader R, Park SH: **Slope-rotatable central composite designs**. *Technometrics* 1978, **20**:413–417.
29. Palasota JA, Deming SN: **Central composite experimental designs: applied to chemical systems**. *J Chem Educ* 1992, **69**:560.
30. Rubin IB, Mitchell TJ, Goldstein G: **Program of statistical designs for optimizing specific transfer ribonucleic acid assay conditions**. *Anal Chem* 1971, **43**:717–721.
31. Baş D, Boyacı IH: **Modeling and optimization I: usability of response surface methodology**. *J Food Eng* 2007, **78**:836–845.
32. Khuri AI, Mukhopadhyay S: **Response surface methodology**. *Wiley Interdiscip Rev Comput Stat* 2010, **2**:128–149.
33. Anderson MJ, Whitcomb PJ: *RSM simplified: optimizing processes using response surface methods for design of experiments*. Virginia: Productivity Pr; 2005.
34. Oehlert GW: *A first course in design and analysis of experiments*. New York: WH Freeman; 2000.
35. Deming S: **Quality by design-part 3**. *Chemtech* 1989, **19**:249–255.
36. Whitcomb PJ, Anderson MJ: *RSM simplified: optimizing processes using response surface methods for design of experiments*. New York: Productivity Press; 2004.
37. Allen DM: **The relationship between variable selection and data augmentation and a method for prediction**. *Technometrics* 1974, **16**:125–127.
38. Stuart A, Ord JK: *Kendall's advanced theory of statistics: vol 1. Distribution theory*. London: Arnold; 1994.
39. Abdollahi Y, Zakaria A, Abdullah AH, Masoumi HRF, Jahangirian H, Shameli K, Rezayi M, Banerjee S, Abdollahi T: **Semi-empirical study of ortho-cresol photo degradation in manganese-doped zinc oxide nanoparticles suspensions**. *Chem Cent J* 2012, **6**:1–8.
40. Box GEP, Wilson K: **On the experimental attainment of optimum conditions**. *J Roy Stat Soc B* 1951, **13**:1–45.
41. Stuart A, Ord JK, Arnold S: *Kendall's advanced theory of statistics: vol 2A. Classical inference and the linear model*. London: Arnold; 1999.

doi:10.1186/1752-153X-7-137

Cite this article as: Abdollahi et al.: Optimizing Bi₂O₃ and TiO₂ to achieve the maximum non-linear electrical property of ZnO low voltage varistor. *Chemistry Central Journal* 2013 **7**:137.

Publish with **ChemistryCentral** and every scientist can read your work free of charge

“Open access provides opportunities to our colleagues in other parts of the globe, by allowing anyone to view the content free of charge.”

W. Jeffery Hurst, The Hershey Company.

- available free of charge to the entire scientific community
- peer reviewed and published immediately upon acceptance
- cited in PubMed and archived on PubMed Central
- yours — you keep the copyright

Submit your manuscript here:
http://www.chemistrycentral.com/manuscript/



ChemistryCentral